THE ASTROPHYSICAL JOURNAL, 471:L5–L9, 1996 November 1

REDSHIFT CLUSTERING IN THE HUBBLE DEEP FIELD[1]

JUDITH G. COHEN,[2] LENNOX L. COWIE,[3] DAVID W. HOGG,[4] ANTOINETTE SONGAILA,[3]
ROGER BLANDFORD,[4] ESTHER M. HU,[3] AND PATRICK SHOPBELL[2]
Received 1996 June 24; accepted 1996 August 14

ABSTRACT

We present initial results from a redshift survey carried out with the low-resolution imaging spectrograph on the 10 m W. M. Keck Telescope in the Hubble Deep Field. In the redshift distribution of the 140 extragalactic objects in this sample, we find six strong peaks with velocity dispersions of ~400 km s^{-1}. The areal density of objects within a particular peak, while it may be nonuniform, does not show evidence for strong central concentration. These peaks have characteristics (velocity dispersions, density enhancements, spacing, and spatial extent) similar to those seen in a comparable redshift survey in a different high Galactic latitude field (Cohen and coworkers), confirming that the structures are generic. They are probably the high-redshift counterparts of huge galaxy structures ("walls") observed locally.

Subject headings: cosmology: observations — galaxies: distances and redshifts — large-scale structure of universe

1. INTRODUCTION

The Hubble Deep Field (HDF) (Williams et al. 1995) has been surveyed to extraordinary depths, with point-source detection limits around 29 mag in the V and I bands, in an intensive campaign by the *Hubble Space Telescope* (*HST*) in 1995 December. The images represent the deepest images ever taken in the optical and have already provided the basis for studies of deep visual counts (Williams et al. 1995), faint object morphology (Abraham et al. 1996), gravitational lensing (Hogg et al. 1996), and high-redshift objects (Steidel et al. 1996; Clements & Couch 1996). These studies represent only the beginning of a large number of scientific projects possible with the HDF data.

In this Letter, we present the first results of a ground-based spectroscopic survey of galaxies in the HDF with the Keck Telescope. These observations were taken in order to provide a database of object redshifts for the use of the astronomical community and in order to expand the faint object redshift surveys of Cowie et al. (1996) and Cohen et al. (1996) to an additional field.

We assume an Einstein–de Sitter universe ($q_0 = 0.5$) with a Hubble constant 100 h km s^{-1} Mpc^{-1}.

2. REDSHIFT SAMPLE

The HDF was selected on the basis of high Galactic latitude, low extinction, and various positional constraints described by Williams et al. (1996). Redshifts were acquired with the low-resolution imaging spectrograph (LRIS) (Oke et al. 1995) on the 10 m W. M. Keck Telescope over two rectangular strips 2×7.3 arcmin^2 centered on the *HST* field in 1996 January, March, and April. One strip was aligned east-west, while the second was aligned at a position angle of 30° in order to maximize the slit length that fell within the HDF itself, where the two strips overlap.

The sample selection is different in each of the two strips. The photometry and the definition of the sample for spectroscopic work are described in Paper II of this series (Cowie et al. 1997). Plans exist to complete the sample in a number of photometric bandpasses, but in view of the great interest in the HDF and the many follow-up studies in progress, we present this data before the complete sample is available.

Table 1 presents the redshifts of 140 extragalactic objects, about half of which are in the HDF itself and the remainder of which in the flanking fields. The median redshift z of the extragalactic objects in the present sample is $z = 0.53$. Only three are quasars or broad-line active galactic nuclei. Twelve Galactic stars were found as well. The radial velocity precision of our redshifts is unusually high for a deep redshift survey. We estimate that the uncertainty in z for those objects with redshifts considered secure and accurate is ≈300 km s^{-1}. Coordinates, crude ground-based R magnitudes in a 3″ diameter intended for object identification only, and redshifts are given in Table 1.

A more detailed account of the photometric and spectroscopic properties of the entire sample, including photometry from U through K, as well as a discussion of incompleteness in the sample selection and redshift identification, is in preparation. These incompletenesses ought not to affect the present work.

3. REDSHIFT DISTRIBUTION

3.1. *Velocity Peaks*

The redshift histogram over the region $0.2 < z < 0.9$ is shown in Figure 1. It shows clear evidence of clustering. Velocity peaks were identified by choosing bins of variable width and centers in such a way as to maximize their significance relative to occurring by chance in a smoothed velocity distribution (smoothing width 20,000 km s^{-1}) derived from the present sample (cf. Cohen et al. 1996). Using this procedure, we isolate six peaks significant at better than 99.5% confidence (see Table 2). The fourth column in Table 2 gives a statistical significance parameter, $X_{\max}$. The fifth and sixth columns give

[1] Based in large part on observations obtained at the W. M. Keck Observatory, which is operated jointly by the California Institute of Technology and the University of California.

[2] Palomar Observatory, California Institute of Technology, 105-24, Pasadena, CA 91125.

[3] Institute for Astronomy, University of Hawaii, 2680 Woodlawn Drive, Honolulu, HI 96822.

[4] Theoretical Astrophysics, California Institute of Technology, 130-33, Pasadena, CA 91125.

TABLE 1

REDSHIFTS IN THE HUBBLE DEEP FIELD

R.A. (-12^h)	decl. ($-62°$)	R_{ap} (3″) (mag)	z	R.A. (-12^h)	decl. ($-62°$)	R_{ap} (3″) (mag)	z	R.A. (-12^h)	decl. ($-62°$)	R_{ap} (3″) (mag)	z
36 21.4	1227.1	...	0.398	36 48.5	1329.2	23.9	0.958	37 01.81	1510.9	22.9	0.938
36 22.0	1237.7	21.7	0.630	36 48.51	1142.3	23.2	0.962	37 02.3	1343.0	21.3	0.559
36 22.2	1241.9	20.8	0.498	36 49.29	1312.3	22.7	0.478	37 02.5	1348.3	22.7	0.513
36 22.7	1300.2	20.0	0.472	36 49.34	1347.9	19.0	0.089	37 02.5	1402.7	22.1	1.243
36 22.9	1346.9	20.4	0.485	36 49.42	1407.8	22.8	0.752	37 02.70	1544.8	20.8	0.514
36 24.9	1301.0	20.3	0.518	36 49.55	1258.8	22.6	0.475	37 02.81	1424.4	21.5	0.512
36 26.5	1252.6	20.6	0.557	36 49.64	1314.2	22.4	0.475	37 03.21	1646.9	23.0	0.744
36 27.7	1241.3	20.8	0.518	36 50.15	1240.8	21.4	0.474	37 03.6	1354.3	21.7	0.745
36 28.1	1238.0	21.1	0.5185	36 50.18	1246.9	22.8	0.680	37 03.82	1442.0	22.3	0.475
36 29.8	1403.8	21.4	0.793	36 50.63	1059.9	21.9	0.474	37 03.91	1523.8	22.6	0.377
36 29.9	1225.0	22.6	0.410	36 50.73	1256.9	23.1	0.320	37 04.17	1625.3	22.8	0.474
36 30.2	1208.8	20.6	0.456	36 51.0	1321.6	20.8	0.199	37 04.52	1652.2	21.1	0.377
36 31.0	1236.9	21.3	0.456	36 51.02	1032.2	21.2	0.410	37 04.56	1430.0	22.0	0.561
36 31.7	1241.1	21.3	0.528	36 51.35	1301.6	22.2	0.089	37 04.73	1455.8	21.2	0
36 32.6	1244.1	21.3	0.562	36 51.61	1221.3	22.3	0.299	37 04.91	1547.4	23.4	0.533
36 33.4	1320.3	21.1	0.843	36 51.69	1354.8	22.0	0.557	37 05.0	1211.2	22.5	0.386
36 33.04	1135.0	19.4	0.080	36 52.03	1458.3	22.4	0.358	37 05.66	1525.7	22.7	0.503
36 33.6	1156.8	21.8	0.458	36 52.39	1036.9	22.2	0.321	37 06.0	1333.9	21.6	0.753
36 34.4	1241.5	22.3	1.219	36 52.59	1221.0	24.0	0.401	37 06.81	1430.3	21.2	0
36 34.8	1224.5	19.5	0.562	36 52.68	1355.7	22.7	1.355	37 07.0	1214.7	21.4	0.655
36 36.1	1320.3	22.1	0.680	36 52.71	1432.9	21.2	0	37 07.0	1158.5	22.4	0.593
36 36.3	1341.2	21.4	0.556	36 52.83	1454.7	22.7	0.463	37 07.73	1606.1	22.8	0.936
36 36.78	1136.1	19.4	0.078	36 52.85	1445.1	20.1	0.322	37 08.01	1631.7	22.7	0
36 37.2	1253.1	20.8	0.485	36 53.33	1235.2	23.4	0.560	37 08.04	1659.6	21.5	0.458
36 37.4	1241.0	20.5	0.458	36 53.54	1526.0	18.7	0	37 08.1	1253.2	21.9	0.838
36 37.6	1149.5	22.1	0.838	36 53.57	1309.4	22.1	0	37 08.1	1321.6	22.7	0.785
36 38.89	1220.7	22.9	0.609	36 53.77	1255.0	22.0	0.642	37 08.20	1454.8	22.8	0.565
36 39.8	1207.5	21.8	1.015	36 54.28	1435.1	22.8	0.577	37 08.25	1515.3	22.5	0.839
36 40.80	1204.4	23.7	1.010	36 54.65	1329.1	20.0	0	37 08.53	1502.2	22.7	0.570
36 41.56	1133.1	20.5	0.089	36 55.44	1354.5	22.4	1.148	37 08.60	1612.4	21.3	0
36 41.85	1206.3	21.9	0.432	36 55.45	1246.4	23.1	0.790	37 08.8	1202.8	22.6	0.855
36 42.85	1217.6	21.3	0.454	36 55.50	1400.9	23.9	0.559	37 09.46	1424.3	22.0	0.476
36 43.07	1243.2	23.0	0.847	36 56.26	1242.4	19.9	0	37 09.79	1525.0	20.0	0.597
36 43.55	1219.4	23.4	0.752	36 56.33	1210.4	23.7	0.321	37 10.1	1320.5	21.7	0.320
36 43.69	1357.7	21.6	0.201	36 56.56	1246.8	21.7	0.5185	37 11.85	1659.7	23.5	1.142
36 43.71	1144.0	22.3	0.765	36 57.14	1227.1	23.4	0.561	37 12.4	1358.2	22.6	0.848
36 43.88	1251.2	21.8	0.557	36 57.22	1300.8	22.3	0.474	37 12.58	1543.4	22.3	0.533
36 44.09	1248.9	22.0	0.555	36 57.64	1316.5	23.8	0.952	37 13.0	1357.2	22.0	1.016
36 44.11	1241.3	24.2	0.873	36 57.98	1301.6	23.0	0.320	37 13.59	1512.0	22.1	0.524
36 44.28	1134.3	23.2	1.013	36 58.22	1215.2	22.9	1.020	37 14.8	1335.4	22.5	0.897
36 44.59	1228.8	24.2	2.268	36 58.29	1549.4	21.7	0.457	37 16.1	1354.2	21.5	0.476
36 45.32	1214.5	21.4	0	36 58.56	1223.0	24.2	0.682	37 16.32	1630.4	23.4	0
36 45.86	1202.4	24.6	0.679	36 58.64	1439.1	23.3	0.512	37 16.4	1311.2	21.9	0.898
36 46.10	1142.9	22.6	1.016	36 58.66	1253.2	22.2	0.321	37 17.0	1357.4	20.7	0.336
36 46.25	1405.6	22.6	0.960	36 58.74	1435.6	21.9	0.678	37 16.52	1644.7	22.7	0.557
36 46.44	1152.3	22.9	0.5035	36 58.76	1638.9	20.0	0.299	37 18.28	1554.1	21.6	0.476
36 46.45	1408.6	23.1	0.130	36 59.43	1222.7	24.5	0.472	37 18.3	1348.6	22.1	0.480
36 46.68	1238.1	23.0	0.320	36 59.79	1450.6	22.5	0.761	37 18.4	1322.5	20.6	0.4755
36 46.78	1145.9	23.1	1.059	37 00.41	1406.7	21.5	0.423	37 18.60	1605.0	22.5	0.558
36 47.21	1231.8	23.4	0.421	37 00.47	1235.9	24.5	0.562	37 22.25	1613.1	22.6	0
36 47.99	1310.1	21.5	0.475	37 01.8	1323.8	20.7	0.408				

NOTE.—Right ascension is in units of minutes and seconds. Declination is in units of arcminutes and arcseconds. Epoch is J2000.

the comoving transverse size corresponding to 1′ and the comoving radial distance corresponding to $\Delta z = 0.001$. The density in velocity space within these peaks exceeds the average density by a factor that ranges from 4 to as high as 30 for the peak at $z_p = 0.321$. Forty percent of the total sample lies within these peaks. Larger peaks including outliers are also highly significant. The local velocity dispersions for these peaks are strikingly small, ranging from 170 to 600 km s^{-1}. These are upper bounds because they are comparable with our measurement errors. They are also similar to the results obtained in a high-latitude field, for which we carried out a deep redshift survey with LRIS earlier (Cohen et al. 1996).

By itself, this sample is too small to measure the two-point correlation function in velocity space. However, there is a 5 σ excess correlation in the 500–1000 km s^{-1} interval with a correlation scale $V_0 \sim 600 \pm 200$ km s^{-1} (cf. Carlberg et al. 1997; Le Fèvre et al. 1996), which can be converted into comoving distance along the line of sight by using the data in the sixth column of Table 2. There is no evidence for correlation with velocity differences in excess of 1000 km s^{-1}. No distinction between low and high redshift is discernible. There is no evidence for periodicity in the peak redshifts (cf. Broadhurst et al. 1990).

3.2. *Morphology Correlation*

If we make a simple morphological separation of the galaxies in the redshift survey into spirals, ellipticals, and

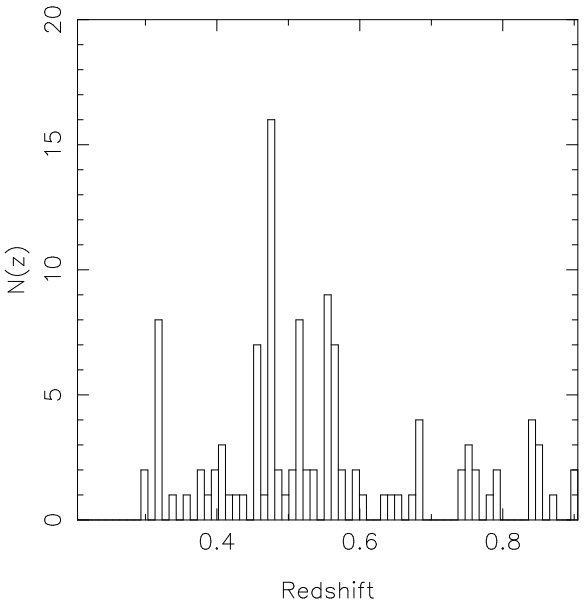

FIG. 1.—Redshift histogram for the galaxies in the merged Caltech and Hawaii survey of the HDF.

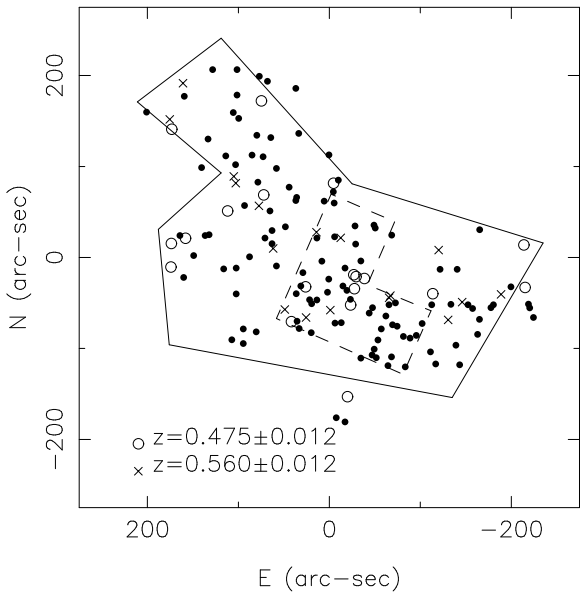

FIG. 2.—Distribution of our sample of galaxies projected onto the sky. Data are from the Caltech and Hawaii survey of the HDF. Galaxies in the two most populous redshift peaks are indicated.

peculiar/mergers, and use the *HST* images of the HDF and of the flanking fields to classify these galaxies (cf. van den Bergh et al. 1996), then we find there is no indication of any difference in population between the background field galaxies and those in the redshift peaks. In particular, the redshift peaks do not contain a detectable excess of elliptical galaxies.

4. ANGULAR DISTRIBUTION

The angular distribution of the entire sample and of the galaxies in the two most populous velocity peaks is shown in Figure 2. The peculiar shape is caused by the use of two LRIS strips with different position angles. The outline of the area covered is indicated by the solid lines, while the outline of the area of the Wide-Field Camera II observations in the HDF is indicated by the dashed lines. The galaxies associated with the six velocity peaks mostly exhibit a nonuniform distribution, though none show the strong central concentration characteristic of clusters. The redshift sample must be completed before it is possible to make quantitative statements.

4.1. *Areal Density*

The areal density of galaxies brighter than $0.1L^*$ (as defined at K) is computed for redshift peaks in the zero-hour field (Cohen et al. 1996) and for the two largest peaks in the HDF, where the K photometry is not fully assembled yet. Corrections have been applied for galaxies below the magnitude cutoff of the survey, assuming a flat luminosity function at the faint end. To investigate a local analog to these structures, this is repeated for the Local Group, for the Virgo Cluster (within a radius of 6° from its center) using the survey of Kraan-Korteweg (1981), and within the core of the Coma Cluster using data from Thompson & Gregory (1980). In these local structures, the luminosity is determined at B rather than at K. The results are given in Table 3 and suggest that the best local analog is the region of the Virgo Cluster within 6° of its center, but although the areal density is a reasonable match, the velocity dispersion in the high-redshift peaks is lower, often significantly lower, than one sees in the central region of the Virgo Cluster.

TABLE 2

REDSHIFT PEAKS IN THE HUBBLE DEEP FIELD

z_p	N[a]	$\sigma_v(N)$[b] (km s^{-1})	$X_{\max}$[c]	$d_\perp(\Delta\theta = 1')$ (h^{-1} Mpc)[d]	$d_\parallel(\Delta z = 0.001)$ (h^{-1} Mpc)[d]
0.321.....	8	170	22	0.22	2.0
0.457.....	7	310	10	0.31	1.7
0.475.....	15	315	21	0.31	1.6
0.516.....	8	595	8	0.33	1.6
0.559.....	14	420	21	0.34	1.5
0.680.....	5	265	8	0.40	1.4

[a] Number of galaxies within the peak, as determined by statistical tests.
[b] No correction for instrumental or measurement errors has been applied.
[c] Statistical parameter for estimating the significance of each peak; see Cohen et al. 1996.
[d] Comoving distances.

5. DISCUSSION

5.1. *Effects of Sample Definition Decisions*

The conclusion of Cohen et al. (1996)—i.e., that a large fraction of the galaxy population at redshifts to unity lie in low velocity dispersion structures—was based on a single field, but the confirmation of strong redshift space clustering in the HDF suggests that the results are generic. The clustering seen here is stronger than that seen in other local and high-redshift surveys (Landy et al. 1996; Le Fèvre et al. 1996). The difference is attributed most importantly to the high sampling density in a small field.

5.2. *Structure Morphology*

At one level, these peaks may be no more than a manifestation of the fact that galaxies are correlated in both configuration and velocity space. The connection between spatial and velocity correlation functions is quite model dependent (e.g., Brainerd et al. 1996). Conversely, if we can gain an empirical understanding of this relationship, it can discriminate among

TABLE 3

AREAL DENSITY OF PEAKS IN THE CALTECH ZERO-HOUR FIELD AND IN LOCAL STRUCTURES

z_p	$N_{obs}(L > 0.1L^*)$	Comoving Area (h^{-2} Mpc^2)	$n_{corr}(L > 0.1L^*)$[a] (h^2 Mpc^{-2})	$\sigma_v(N\text{-}1)$ (km s^{-1})
0.392.....	3	1.03	3	465
0.429.....	14	1.19	13	615
0.581.....	23	1.86	19	410
0.675.....	8	2.30	7	405
0.766.....	7	2.72	7	670
0.475 (HDF)[b]	7	0.51	18	315
0.559 (HDF)[b]	7	0.64	17	420
Local Structures				
Local Group	4	1.3	3[c]	<100
Virgo[d]	122	8.5	14[c]	670[e]
Coma[f]	248	2.0	125	1080[g]

[a] Comoving areal density corrected for incompleteness at the faint end.
[b] The area is that of the three Wide-Field CCDs.
[c] Independent of h.
[d] Galaxies within a 6° radius of the cluster center.
[e] Bingelli, Sandage, & Tammann 1985.
[f] Galaxies within the central region 1.°2 on a side.
[g] Colless & Dunn 1996 (square region 2.°6 on a side).

cosmogonic models. We briefly comment upon some possibilities.

One explanation is that the velocity peaks represent structures in velocity space and are not prominent in real space. Such effects are sometimes seen in numerical simulations (e.g., Park & Gott 1991; Bagla & Padmanabhan 1994). For example, they might be a "backside infall" into a large structure in which the Hubble expansion opposes the infall so as to give more or less uniform recession velocity over a large interval of radial distance. The generic kinematic difficulty with this explanation is that in order for features like this not to have many more descendants in which the velocities have long ago crossed, the characteristic lifetimes must be a significant fraction of the age of the universe, which, in turn, limits the mass density contrast to small values. Given that half the galaxies lie in these structures, a large bias parameter must be invoked.

Alternatively, we may be observing structures that are spatially compact and have the shapes of spheres, filaments, or walls. We can argue against these features being clusters on the following grounds: (1) they do not exhibit central concentrations (cf. § 4); (2) the velocity dispersions are too small, 200–600 km s^{-1} as opposed to 600–1200 km s^{-1}; (3) the space density of rich clusters is too low—the Palomar Deep Cluster Survey (Postman et al. 1996) finds only seven clusters per square degree out to $z \sim 0.6$ with richness class ≥ 1; and (4) the redshift peaks do not show the excess of ellipticals characteristic of rich clusters (Dressler 1980).

Small quasi-spherical groups are a possibility. The mean free path is $\sim 100\ h^{-1}$ comoving megaparsec. The observed structures extend laterally over at least $\sim 6'$ or $\sim 2\ h^{-1}$ Mpc, implying a space density $\sim 3 \times 10^{-3}\ h^3$ Mpc^{-3}, about one-third the density of L^* galaxies. Alternatively, we can associate the tentative velocity correlation scale of $V_0 \sim 600$ km s^{-1} with a radial extent of $\sim 4\ h^{-1}$ Mpc and a lateral angular scale of $\sim 12'$ at $z \sim 0.5$.

Filaments and walls have both been described in the theoretical literature (e.g., Bond, Kofman, & Pogosyan 1996; Shandarin et al. 1995). Walls dominate if there is excess power on large scales and they are observed locally (e.g., in the Local Supercluster, de Vaucouleurs 1975; and in local redshift surveys, de Lapparant, Geller, & Huchra 1986; Landy et al. 1996). On this basis, we speculate that the structures we are observing are actually walls.

There are two obvious follow-up investigations that can address this hypothesis. The first is to perform similar redshift surveys in neighboring deep fields. If we assume that the wall normal is inclined at an angle θ to the line of sight and that the constituent galaxies move with the Hubble flow in two dimensions, then the variation of mean redshift with angular separation of the second survey $\Delta\phi$ and polar angle on the sky ψ is

$$\Delta z = 2[(1 + z)^{3/2} - (1 + z)]\Delta\phi \tan\theta \sin\psi .$$

For $z = 0.5$, this is $\Delta z \sim 2 \times 10^{-4}$ arcmin^{-1}, and in order to see redshift displacements in excess of the velocity dispersion the additional surveys must be displaced by $\sim 20'$. With several lines of sight, it might be possible to test the above relation.

The second approach is to look for morphological and luminosity function differences between the galaxies within and outside the velocity peaks using wide-field, multiband photometric surveys to the depth of the redshift survey. Both investigations are underway.

We thank the Hubble Deep Field team, led by Bob Williams, for planning, taking, reducing, and making public the HDF images. We are grateful to George Djorgovski, Keith Matthews, Gerry Neugebauer, Paddy Padmanabhan, Mike Pahre, Tom Soifer, and Jim Westphal for helpful conversations. The entire Keck user community owes a huge debt to Bev Oke, Jerry Nelson, Gerry Smith, and many other people who have worked to make the Keck Telescope a reality. We are grateful to the W. M. Keck Foundation, and particularly its president, Howard Keck, for the vision to fund the construction of the W. M. Keck Observatory. Support by NASA and the NSF is greatly appreciated.

REFERENCES

Abraham, R. G., Tanvir, N. R., Santiago, B. X., Ellis, R. S., Glazebrook, K., & van den Bergh, S. 1996, MNRAS, 279, L47
Bellanger, C., & de Lapparent, V. 1995, ApJ, 455, L103
Binggeli, B., Sandage, A., & Tammann, G. A. 1985, AJ, 90, 1681
Bond, J. R., Kofman, L., & Pogosyan, D. 1996, Nature, 380, 603
Brainerd, T. G., Bromley, B. C., Warren, M. S., & Zurek, W. H. 1996, ApJ, 464, L103
Broadhurst, T., Ellis, R., Koo, D., & Szalay, A. 1990, Nature, 343, 726
Carlberg, R. G., Cowie, L. L., Songaila, A., & Hu, E. M. 1997, in press
Clements, D. L., & Couch, W. J. 1996, MNRAS, 280, L43
Cohen, J. G., Hogg, D. W., Pahre, M. A., & Blandford, R. 1996, ApJ, 462, L9
Colless, M., & Dunn, A. M. 1996, ApJ, 458, 435
Cowie, L. L., et al. 1997, in preparation
Cowie, L. L., Songaila, A., Hu, E. M., & Cohen, J. G. 1996, AJ, in press
de Lapparent, V., Geller, M., & Huchra, J. P. 1986, ApJ, 302, L1
de Vaucouleurs, G. H. 1975, in Galaxies and the Universe, ed. A. Sandage, M. Sandage, J. Kristian, & G. Tammann (Chicago: Univ. Chicago Press), 557
Dressler, A. 1980, ApJ, 236, 351
Hogg, D. W., Blandford, R. D., Kundić, T., Fassnacht, C. D., & Malhotra, S. 1996, ApJ, 467, L73
Kraan-Korteweg, R. 1981, A&A, 104, 280
Landy, S. D., Shectman, S. A., Lin, H., Kirshner, R. P., Oemler, A. A., & Tucker, D. 1996, ApJ, 456, L1
Le Fèvre, O., Hudon, D., Lilly, S. J., Crampton, D., Hammer, F., & Tresse, L. 1996, ApJ, 461, 534
Oke, J. B., et al. 1995, PASP, 107, 3750
Park, C. B., & Gott, J. R. 1991, MNRAS 249, 288
Postman, M. A., Lubin, L. M., Gunn, J. E., Oke, J. B., Hoessel, J. G., Schneider, D. P., & Christensen, J. A. 1996, AJ, 111, 615
Shandarin, S. F., Melott, A. L., Mcdavitt, K., Pauls, J. L., & Tinker, J. 1995, Phys. Rev. L, 75, 7
Steidel, C. C., Giavalisco, M., Dickinson, M., & Adelberger, K. L. 1996, AJ, 112, 352
Thompson, L. A., & Gregory, S. A. 1980, ApJ, 242, 1
van den Bergh, S., Abraham, R. G., Ellis, R. S., Tanvir, N. R., & Santiago, B. X. 1996, AJ, 112, 359
Williams, R. E., et al. 1996, AJ, in press.